# The diversity of radial variations of wood properties in European beech reveals the plastic nature of juvenile wood

Tancrède Alméras, Delphine Jullien, Shengquan Liu, Caroline Loup, Joseph Gril, Bernard Thibaut

# The diversity of radial variations of wood properties in European beech reveals the plastic nature of juvenile wood

ALMERAS Tancrède[1], JULLIEN Delphine[1], LIU Shengquan[2], LOUP Caroline[3], GRIL Joseph[4,5,*], THIBAUT Bernard[1]

[1] LMGC, Univ Montpellier, CNRS, Montpellier, France
[2] School of Forestry & Landscape Architecture, Anhui Agricultural University, Hefei, China.
[3] Service du Patrimoine Historique, Univ Montpellier, Montpellier, France
[4] Université Clermont Auvergne, CNRS, Institut Pascal, Clermont-Ferrand, France
[5] Université Clermont Auvergne, INRAE, PIAF, Clermont-Ferrand, France
* Corresponding author, email: joseph.gril@cnrs.fr

**Keywords**

Beech; Wood properties; Variability; Radial variation; Juvenile transition; Ontogenetic juvenility; Adaptive juvenility

**Abstract (401 words)**

The long-term radial variation of wood properties from pith to bark are largest in the young ages of the tree (internal core). This so-called juvenility reflects both cambium ageing (ontogenetic juvenility) and adaptation to the changing mechanical constraints during secondary growth (adaptive juvenility). Ring width (*RW*), specific gravity (*SG*) and specific modulus (*SM*) are important parameters for each new wood layer, needed for the study of mechanical stability of a standing tree. They should be sensitive to the mechanical adaptation of growth. They were measured on diametrical boards (North/South direction) issued from 86 trees from several high forest stands in European countries. Analysis of variance showed very significant influence of position within the tree (core/external), of trees within a plot and of plots, but not for North/South orientation. The share of variance was similar for *SG* and *SM* (importance of tree effect) but different for *RW* (importance of plot effect). The occurrence of red heartwood in the core on some trees had a significant influence, mostly on *SM*, but the differences between white and red wood was very small. Globally the variability is high for *RW*, rather small for *SM* and very small for *SG*. Accordingly, the variations of the modulus of elasticity (product of *SG* and *SM*) were much more influenced by *SM* than by *SG* for beech. The radial variations of each parameter were fitted by both a linear (2 coefficients: zero value and mean slope) and a parabolic curve (3 coefficients: zero value, initial slope and curvature). They were used to classify types or radial profile in terms of flat, up & down and straight, convex & concave. Median values of coefficients per plot (or total) were used to draw median profiles for each parameter per plot and at the global level. The median global profiles differ from the typical radial pattern (TRP) of juvenility for plantation softwoods for *SG* (down concave instead of up concave) and *SM* (convex as TRP but with a clear decrease in the mature wood). The main result was the very large variability of profiles between trees or even between plots. Even if there is a part of ontogenetic influence in the juvenile patterns for *RW*, *SG* and *SM*, the results suggest that the influence of mechanical constraints in the tree growth (adaptive juvenility) dominates largely.

## Notations and abbreviations

| | |
|---|---|
| *CV* | coefficient of variation |
| *D* | density |
| L, *L* | longitudinal direction, specimen length in L direction |
| R, *R* | radial direction, specimen length in R direction |
| *RW* | ring width |
| *SG* | specific gravity (ratio of *D* over water density) |
| *SM* | specific modulus (squared value of sound speed in L direction) |
| T, *T* | tangential direction, specimen length in T direction |
| TRP | typical radial pattern |
| *W* | specimen weight |

## 1. Introduction

Wood is an adaptation to the competition for height growth in the terrestrial environment, which is submitted to tremendous physical constraints such as gravity, wind and drought. The functions of wood (mechanical support, conduction and storage) respond these constraints, and are fulfilled by different cell types (fibres or tracheids, vessels and parenchyma). In tree species, the bulk of wood material is generally made of fibres, which have mainly a mechanical function. Despite their major importance for tree functioning and survival, other cell types generally represent only a small part of wood in terms of biomass investment. Actually, most of terrestrial biomass is in the form of fibres (Bar-on et al 2017). This massive investment in fibres points to the major significance of the mechanical constraint for trees. The viewpoint that we will adopt here is that wood production quantity and quality are mainly responses to the mechanical requirement of the tree to face the two major constraints that are wind and gravity.

Trees are built through wood growth (Thibaut 2019) including simultaneously primary growth by elongation or creation of twigs and secondary growth by thickening of existing axes. Secondary growth is performed by living wood cells in the cambial zone: stem cells of cambium itself and daughter cells (Raven et al 2007, Savidge 2003, Déjardin et al 2010, Thibaut 2019). It consists of the following successive steps: division of the cambium stem cells into daughter cells; expansion of daughter cells until the end of primary wall formation; thickening of the fibre (or tracheid) cell walls until the end of secondary wall formation; lignification of the whole cell wall, including the compound middle lamella; programmed fibre and vessel cell death.

During this cambial activity, wood features are achieved. They can be described by ring width (*RW*), result of combined cell division and expansion, specific gravity (*SG*) resulting from the ratio between cell wall thickening and expansion, and specific modulus (*SM*) mainly determined by the organisation of the secondary cell wall (micro-fibril angle of the S2 layer) (Cave 1969). These three features determine most parameters involved in the adaptation to mechanical constraints. For a trunk of a given height, the rigidity against lateral wind forces depends on trunk diameter (related to *RW*) and on wood modulus of elasticity (MOE) which is the product of SG and SM (Fournier et al. 2013). For a given biomass investment, there is a trade-off between *RW* (large growth rate) and *SG* (large density). The flexibility of the trunk depends inversely on diameter, and positively on wood deformability (equal to the ratio of strength to modulus of elasticity, which is negatively correlated to *SM* as can be seen on wood database, e.g. Ross 2010). The mechanical stability of the tree depends on its diameter, modulus of elasticity (product of *SG* by *SM*), and inversely on its green density (correlated to *SG*, Dlouha et al 2018). The postural control (Alméras & Fournier 2009) depends on the asymmetry in radial growth rate (related to *RW*), modulus of elasticity, and maturation strain (often correlated to *SM*, Alméras et al 2005). Mechanical adaptation is therefore a matter of fine-tuning of wood properties, accounting for the trade-offs between them.

The secondary growth descriptors (*RW*, *SG*, *SM*) display spatial variation within a portion of trunk, in the 3 cylindrical directions: transversely across radii (Tar), around the perimeter (Ap) and longitudinally along the stem (Las), called variation "TarApLas" within the tree by Savidge (2003). The variations around the perimeter in a given ring are related to posture control (Alméras and Fournier 2009), either due to trunk inclination (Alméras et al 2005, Dassot et al. 2015) or to orientation change of the branches after apex death (Loup et al 1991). The variations along the stem deal with primary growth: i) succession of connected zones and free-from-branching portions of the axis and ii) ageing of the terminal bud in the successive growth units. Apart from the vicinity of the branching zones, these variations are rather slow (Savidge 2003).

Radial variations from pith to bark at a given height can be divided in two types: i) intra-ring short distance changes mostly due to seasonal effects and ii) variations of mean ring properties, reflecting adaptations to changes in mechanical constraints during ontogeny. These mechanical constraints change according to the size of the tree (Fournier et al. 2013). The biggest variations in dimensions and environment occur during the young ages, and so are the variations of wood properties showing higher radial gradients in the inner part of the axis, called *juvenile wood* or core wood depending on the authors (Lachenbruch et al 2011).

A good description of that is given in Bendtsen & Senft (1986). Loblolly pine (Fig. 1 and Fig. 2) is an example of the typical radial pattern (TRP) of juvenility (Lachenbruch et al 2011): initial increase of tracheid length, specific gravity (*SG*) and specific modulus (*SM*), initial decrease of ring width (*RW*). The initial increasing or decreasing portion called juvenile wood is followed by a more or less constant value called mature wood. This is the general case in softwood plantation trees (Cown & Dowling 2015, Larson et al 2001).

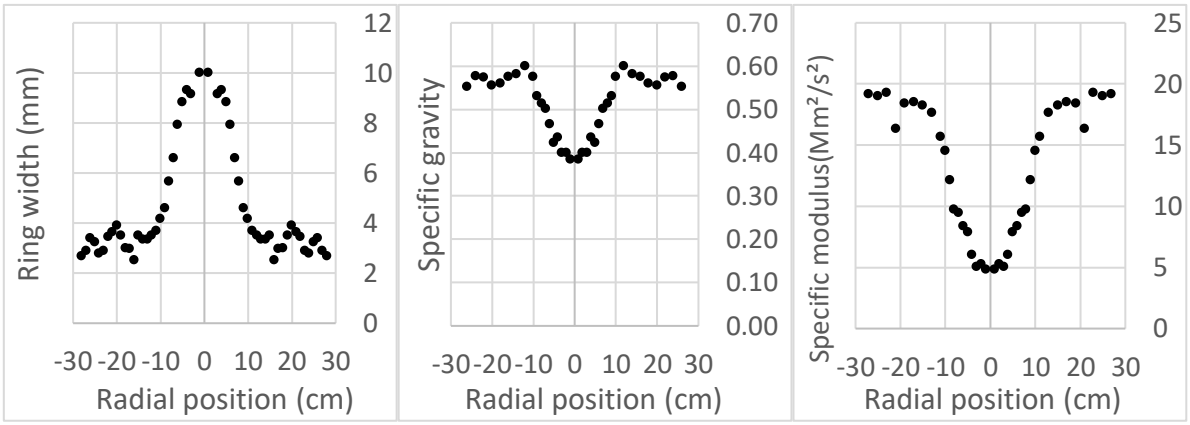


Fig. 1. Juvenility for mechanical indicators (typical radial patterns), after Bendtsen & Senft (1986). Ring width in mm; specific modulus in $10^6$ m²/s

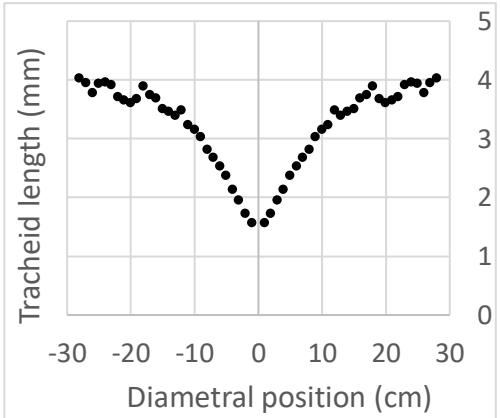


Fig. 2. Juvenility for tracheid length (after Bendtsen & Senft 1986)

Variations in tracheid or fibre length always share the same initial positive gradient for all trees (Fig. 2), whether softwood or hardwood (Koubaa et al 1998, Larson et al 2001, Bhat et al 2001, Bao et al 2001, Kojima et al 2009). This parameter is important for paper industry (Koubaa et al 1998) but is not cited as a factor influencing wood mechanical properties (Kollmann & Côté 1968, Kretschman 2010).

The variation of parameters characterizing wood structure and properties depends on tree ontogeny and adaptation to changing constraints during its life. *Juvenility* describes the evolution of wood parameters during the early years of the stem. An important question is to separate the genetically programmed changes in properties with ontogeny (here termed *ontogenetic juvenility*) from the plastic adaptation to changing constraints (here termed *adaptive juvenility*). The systematic nature of juvenile gradients in fibre length suggest that they are consequence of cambium ageing (ontogenetic juvenility). Here we aim at investigating whether juvenile variations in 3 functional wood properties (*RW*, *SG* and *SM*) depend on plastic adaptation or on prescribed ontogenetic changes.

The data obtained on a large panel of beech trees will be exploited to characterize the patterns of radial variations of wood mechanical indicators in beech. Hypotheses that will be discussed are the following: i) most of the variation are similar all around the trunk (profile symmetry), ii) all the trees share the same radial pattern (ontogenetic juvenility) within the different growing conditions.

In healthy beech trees, heartwood and sapwood can scarcely be distinguished. A so-called “red heartwood”, which is a kind of chemical discoloration, is often observed (Liu et al 2005) and it affects the commercial value of the products (Trenčiansky et al 2017). The hypothesis that red wood occurrence does not affect mechanical parameters will also be tested.

## 2. Material and methods

### *2.1. Material*

Nine plots representative of forest management in Western Europe (Becker & Beimgraben 2001, Jullien et al 2013) were selected (Table 1). The objective was not to study the role of forest management but to have a sufficient diversity of growth history. Up to ten trees per plot (86 in total) were selected for the measurement of wood properties (Table 1). All trees were dominant or co-dominant and their mean diameter at breast height was around 60 cm (Table 2).

Table 1. Characteristics of the studied plots

| | age (years) | Plot | | | | | | | | |
|---|---|---|---|---|---|---|---|---|---|---|
| | | 1 | 2 | 3 | 4 | 5 | 6 | 7 | 8 | 9 |
| Forest: | Nb trees | 10 | 10 | 10 | 10 | 10 | 8 | 10 | 10 | 8 |
| Even-aged | 100-130 | o | | o | o | o | o | | | |
| Even-aged (mountain) | 120-150 | | o | | | | | | o | |
| Uneven-aged | 60-120 | | | | | | | o | | |
| Middle to even-aged forest | 60 | | | | | | | | | o |
| Height | m | 32.6 | 32.1 | 35.5 | 36.1 | 36 | 38.3 | 34 | 39.2 | 35.3 |
| Slenderness | m/m | 58.3 | 65 | 58.9 | 64 | 64.9 | 61.7 | 60.2 | 68 | 47.6 |
| DBH | cm | 56 | 49.4 | 60.7 | 56.6 | 55.4 | 62.5 | 56.9 | 58.2 | 74.5 |

Table 2. Geometric description of the 86 selected trees

| 86 trees | Mean | Min | Max | CV |
|---|---|---|---|---|
| Height (m) | 35.4 | 23.7 | 42.6 | 10.1% |
| Slenderness (m/m) | 61.3 | 41.0 | 80.4 | 13.2% |
| Diameter (cm) | 58.5 | 47.0 | 84.5 | 13.2% |

Min: minimum value; max: maximum value; CV: coefficient of variation

One small log of 50 cm length was cut at a height of 4 m for each tree. Each small log was cut into radial boards, through the pith, from North to South (North direction was carved in the log bark). These boards were air-dried to an average moisture content of 13.5 % and cut into 1259 rods of 20 mm in radial, 20 mm in tangential and 360 mm in longitudinal direction, from the pith outwards (Fig. 3). The rods with irregularities or cracks were discarded.

The rods were numbered according to their position in the board, their distance to pith was measured, and their orientation (North or South) was noted. At the same time, the number of rings at both ends of the samples was recorded and the mean annual ring width of the rod (*RW*) was calculated as the ratio of the mean radial dimension to the number of rings. Each sample located at a distance lower than 10 cm from the pith was considered as a "core" sample. The presence of red heartwood was also noted for the rods located in the core, in relation to a previously published work (Liu et al 2005).

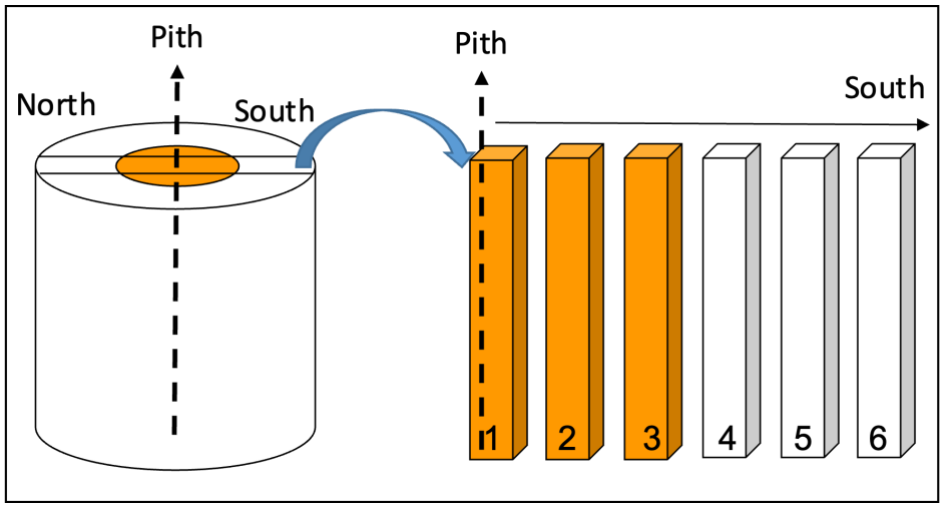


Fig. 3. Diagram of the sawing of the rod after the sawing of a North-South diametrical board. Numbering both for Northern and Southern parts of the board start with pith position. The coloured parts evoke the case of red heartwood occurrence.

### *2.2. Measurement of properties.*

The density (*D*) was calculated by measuring the weight (*W*) and the dimensions *R*, *T*, *L* of the rod in direction R, T, L, respectively: $D = W/(R.T.L)$. The specific gravity (*SG*) was the ratio between *D* and water density.

To measure the specific modulus (*SM*, $10^6 m^2/s^2$), each rod was positioned on fine wires and set in free vibration by a hammer stroke. The analysis of the sound vibration by fast Fourier transform gave the values of the three highest resonance frequencies, which were interpreted using Timoshenko solution (Brancheriau & Baillères 2002).

### *2.3. Statistical analyses*

#### 2.3.1 Correlations and basic statistics

Basic statistical analyses were performed using XLSTAT software. The data description table included the number of data, the minimum, maximum and mean values for each parameter, as well as the coefficient of variation (*CV*). The normality of the distribution was verified by Shapiro-Wilk test. A Pearson correlation analysis was used in the case of a normal distribution, and a Spearman correlation analysis in the case of a non-normal distribution, which was the majority of cases.

#### 2.3.2 Analysis of variance and variance components

Analyses of variance (ANOVA) and variance components analyses (VCA) were carried out using R software (R Core Team 2018). A first set of analyses tested the effect of the different factors on the three measured variables (*RW*, *SM* and *SG*), using a nested ANOVA design where a random "tree" factor was nested within the "plot" factor, and the "core" factor nested within the "tree" factor. Sample orientation (North or South) was accounted for through an independent "orientation" factor.

Another set of ANOVA and VCA was carried out to test the effect of red heartwood on wood properties. This analysis was based only on core specimens, as red heartwood occurs only on these specimens. As both the measured properties and the occurrence of red heartwood were correlated to the distance to the pith (red heartwood occurs more often in inner parts of the core), its effect was tested with a two-ways ANOVA, with specimen number and red heartwood occurrence (Red) as two independent factors. A VCA was carried out on this model to quantify the share of variance of each factor.

#### 2.3.3 Quantitative analysis of radial profiles

North and south radial profiles were analysed together, yielding 172 profiles on which the three variables (*RW*, *SG* and *SM*) have been quantified as a function of the distance to the pith. We built a Microsoft Excel file to view and analyse these profiles (see Suppl. Mat.). The purpose of this analysis was the quantification of the shapes of these profiles, and how they correlate between properties or vary between plots. To achieve this, we considered two main indicators of each profile's shape: the slope, and the curvature.

The slope of the particular radial profile was computed as the coefficient of the linear regression between the considered property and the distance to the pith. It indicates whether the property is globally increasing, decreasing, or staying constant. The curvature was computed as the coefficient of quadratic term of a second-degree polynomial regression. A positive value corresponds to a convex shape, where the local slope increases outward, whereas a negative value corresponds to a concave shape, where the slope decreases outward. All combinations of slope and curvature can exist. Thus, each profile could be represented as a dot on a slope/curvature graph, corresponding to a particular shape. The correspondence between parameter's values and profile shapes is illustrated on Fig. 4, where the 'icons' illustrate the symmetric shape corresponding to their position on the graph.

The correlations between quantitative parameters of the profiles were studied through a PCA (carried out using R) taking into account the following 15 variables for each of the 172 radial profiles: the mean value of the property (*RW_m*, *SG_m*, *SM_m*), the global slope (*RW_s*, *SG_s*, *SM_s*) obtained from the linear regression, the initial value of the property (*RW_a0*, *SG_a0*, *SM_a0*), the initial slope of the property (*RW_a1*, *SG_a1*, *SM_a1*) and the curvature (*RW_a2*, *SG_a2*, *SM_a2*), obtained as the coefficients of the second-degree polynomial regression.

At the plot level, we computed the median and the interquartile range of each parameter (slope and curvature) on each variable (*RW*, *SG* and *SM*), to appreciate whether there were systematic

differences in profile shapes between plots. An ANOVA was used to test the effect of the plot factor on each parameter.

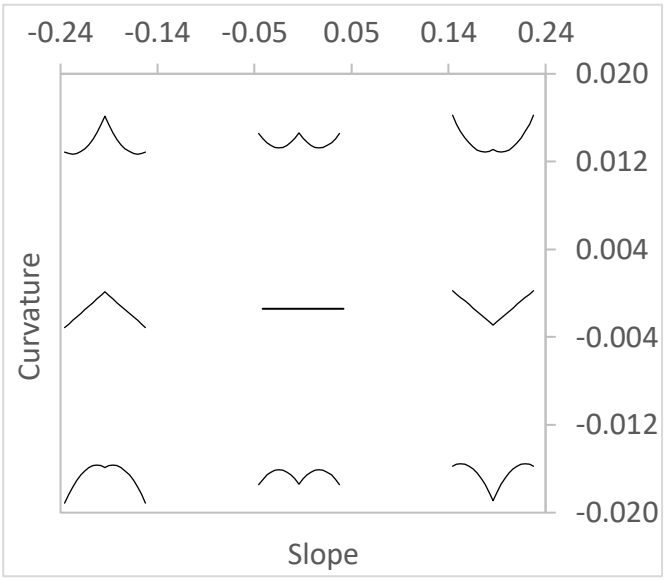


Fig. 4. Illustration of the correspondence between profile parameters (slope and curvature) and shape of a symmetric profile ("flying bird" icons).

The 172 profiles were then classified according to two criteria: they were classified as "Flat", "Up" or "Down" according to a threshold on the slope, and as "Straight", "Convex" or "Concave" according to a threshold on the curvature. We used a criterion based on the magnitude of the effect of each parameter rather than on its statistical significance. Indeed, in many cases the significance of the slope (or curvature) was found high (low P-value) although the magnitude of the effect was weak when compared to the overall range of variation of the parameter. The threshold values were set at an arbitrary 50% of the overall standard deviation of each variable, scaled by the mean distance to the pith (10 cm) for the slope, and by its square for the curvature. At the tree level, the diametral profiles (including both north and south profiles) were classified as symmetric ("Sym") if parameters of the North and South profiles differed less than a threshold defined consistently with above (see suppl. mat.).

## 3. Results

### *3.1 Structuration of variance at the within-tree, between-tree and between-plot levels*

ANOVA was highly statistically significant on each of the three measured variables (*RW*, *SG* and *SM*). Plot, tree within plot and core within tree were all very highly significant factors ($P < 10^{-6}$) for the three variables, while orientation was a significant factor only for *SM* ($P = 0.00012$). The share of variance of each factor for each variable is displayed in Table 3, together with the statistical significance of each factor. For *RW*, the core factor (inner 10 cm radius, compared to the outer zone) represented the largest part of variance, followed by the plot and tree factors. For *SG* and *SM*, the tree factor was the largest part of variance. The orientation factor was statistically significant only for *SM* with a very low share of variance and a very low difference in mean value for North (637 rods; mean value = 22.1 $10^6$ m²/s²) and South (622 rods; mean value = 22.4 $10^6$ m²/s²).

Table 3. Results of the variance component analysis of the effect of Plot, Tree, Core and Orientation factors on the properties of all specimens: share of variance for each factor (%) and significance of the factors

| Factor | *RW* | *SG* | *SM* |
|---|---|---|---|
| Plot | 21.9*** | 14.0*** | 15.4*** |
| Plot/tree | 9.2*** | 36.4*** | 28.6*** |
| Plot/tree/core | 29.5*** | 18.2*** | 14.6*** |
| Orientation | ns | ns | 0.8*** |

*** P<$10^{-3}$; ns P>0.05; *RW*: ring width; *SG*: specific gravity; *SM*: specific modulus

The effect of red heartwood on wood properties was tested on core specimens only, accounting for the distance to the pith (specimen number) as an independent factor. The results (Table 4) show that the distance to the pith was always a significant factor while red heartwood was non-significant for *RW* and *SG*.

Table 4. Results of the variance component analysis of the effect of red heartwood occurrence (Red) and specimen number (Num, indicating the distance to the pith) on the properties of core specimens: share of variance for each factor (%) and significance of the factors

| Factor | *RW* | *SG* | *SM* |
|---|---|---|---|
| Num | 2.5** | 2.7*** | 3.0*** |
| Red | ns | ns | 8.6*** |

*** P<$10^{-3}$; ** P<$10^{-2}$; ns P>0.05; *RW*: ring width; *SG*: specific gravity; *SM*: specific modulus

### *3.2. Correlations between properties at different levels*

Ring width, specific gravity and specific modulus play a role in stem construction and are linked to the 3 successive phases of living wood cells in the cambial zone: cell division, cell expansion and cell-wall thickening. Each phase is influenced by the mechanical and hydraulic constraints on the tree during wood growth. So, it is rather doubtful that the variation of the three mechanical parameters are independent. Distribution of properties and correlations between them can be computed at each level (between rods, between trees and between plots). It is expected that the variability of properties decreases between the rod, tree and plot levels.

#### 3.2.1. Rod level

Table 5 shows descriptors of the distribution of properties for all samples (1259 rods). The variation of *SG* between samples was very low (coefficient of variation 6.2%) compared to that of *SM* (10.9%) and *RW* (35%).

Table 5. Parameter description for all rods

| 1259 rods | *RW* | *SG* | *SM* |
|---|---|---|---|
| Minimum | 0.67 | 0.55 | 11.08 |
| Maximum | 6.67 | 0.83 | 27.49 |
| Mean | 2.30 | 0.69 | 22.22 |
| Max/min | 10.00 | 1.51 | 2.48 |
| C.V. | 35.0% | 6.2% | 10.9% |

*RW*: ring width (mm); *SG*: specific gravity; *SM*: specific modulus ($10^6 m^2/s^2$)

Table 6. Correlation table for all rods (Spearman)

| 1259 rods | *RW* | *SG* | *SM* |
|---|---|---|---|
| RW | 1 | 0.16*** | -0.33*** |
| SG | 0.16*** | 1 | 0.12*** |
| SM | -0.33*** | 0.12*** | 1 |

*RW*: ring width; *SG*: specific gravity; *SM*: specific modulus

*SG* and *SM* were correlated positively (Table 6). *RW* was correlated positively with *SG* and negatively with *SM*. These correlations were very significant (below the 0.1% level) although they were quantitatively rather weak, explaining only 5% to 10% of variance.

### 3.2.2. Tree level

Table 7 shows the descriptors of the distribution of mean values of properties per tree. Variability at the tree level, as quantified by the coefficients of variation, was significantly lower than for the rod level, and notably low for *SG*. This result was consistent with the fact that a substantial part of the variance was at the within-tree level (Table 3, "Core" factor).

At the between-tree level, only the negative correlation between *RW* and *SM* remained significant (Table 8), showing that trees with higher growth rates (higher mean *RW*) had lower *SM*. Note that the correlation between these properties was even higher in magnitude at the tree level (-0.40) than at the rod level (-0.33).

Table 7. Parameter description for tree mean values

| 86 trees | *RW* | *SG* | *SM* |
|---|---|---|---|
| Minimum | 1.29 | 0.63 | 17.6 |
| Maximum | 4.78 | 0.78 | 25.6 |
| Mean | 2.28 | 0.70 | 22.4 |
| Max/min | 3.70 | 1.24 | 1.46 |
| C.V. | 24.9% | 4.8% | 7.6% |

*RW*: ring width (mm); *SG*: specific gravity; *SM*: specific modulus ($10^6 m^2/s^2$)

Table 8. Correlation table for all trees (Spearman)

| 86 trees | *RW* | *SG* | *SM* |
|---|---|---|---|
| *RW* | **1** | $0.08^{ns}$ | $-0.40^{***}$ |
| *SG* | $0.08^{ns}$ | **1** | $0.16^{ns}$ |
| *SM* | $-0.40^{***}$ | $0.16^{ns}$ | **1** |

*RW*: ring width; *SG*: specific gravity; *SM*: specific modulus

### 3.2.3. Plot level

Table 9 shows the descriptors of the distribution of mean values of properties per plot. Variability at the plot level, as quantified by the coefficients of variation, was significantly lower than for the tree level, consistent with the large part of variance at the between-tree level (Table 3, "Tree" factor).

Table 9 Parameter description for the 9 plots mean values

| Plot | *RW* | *SG* | *SM* |
|---|---|---|---|
| 1 | 2.06 | 0.70 | 21.5 |
| 2 | 1.80 | 0.71 | 23.1 |
| 3 | 2.63 | 0.70 | 22.2 |
| 4 | 2.50 | 0.71 | 21.2 |
| 5 | 2.12 | 0.68 | 21.9 |
| 6 | 2.57 | 0.73 | 23.7 |
| 7 | 2.84 | 0.68 | 22.0 |
| 8 | 1.63 | 0.68 | 24.1 |
| 9 | 2.50 | 0.67 | 21.7 |
| Maximum | 2.84 | 0.73 | 24.1 |
| Minimum | 1.63 | 0.67 | 21.2 |

| | | | |
|---|---|---|---|
| Mean | 2.29 | 0.70 | 22.4 |
| C.V. | 16.9% | 2.6% | 4.2% |

*RW*: ring width (mm); *SG*: specific gravity; *SM*: specific modulus ($10^6 m^2/s^2$)

At the plot level there were no more significant correlation between indicators (Table 10).

Table 10. Correlation table for all plots (Spearman)

| 9 Plots | *RW* | *SG* | *SM* |
|---|---|---|---|
| *RW* | **1** | $0.18^{ns}$ | $-0.17^{ns}$ |
| *SG* | $0.18^{ns}$ | **1** | $0.23^{ns}$ |
| *SM* | $-0.17^{ns}$ | $0.23^{ns}$ | **1** |

*RW*: ring width; *SG*: specific gravity; *SM*: specific modulus

### *3.3. Diversity of radial profiles of properties*

#### 3.3.1 Illustration of profile diversity

A total of 516 profiles (86 trees x 2 orientations x 3 variables) were observed and analysed. The mean coefficients of determination ($R^2$) of the regressions was 0.43 for linear regression, and 0.61 for second-degree polynomial regressions, showing that the quadratic term captured a large part of profile non-linearity.

Examples of typical profiles together with the second-degree fitting are shown in Fig. 5 (all profiles can be viewed from the file provided as supplementary material). The chosen examples illustrate the diversity of the diametral profiles, with symmetric profiles (a, b, c, e) as well as non-symmetric profiles (d, f). The radial profiles were either flat (a), increasing (c, d, e-South, f) or decreasing (b), and either straight (a, c, d-North), convex (b, f-North) or concave (d-South, e, f-South).

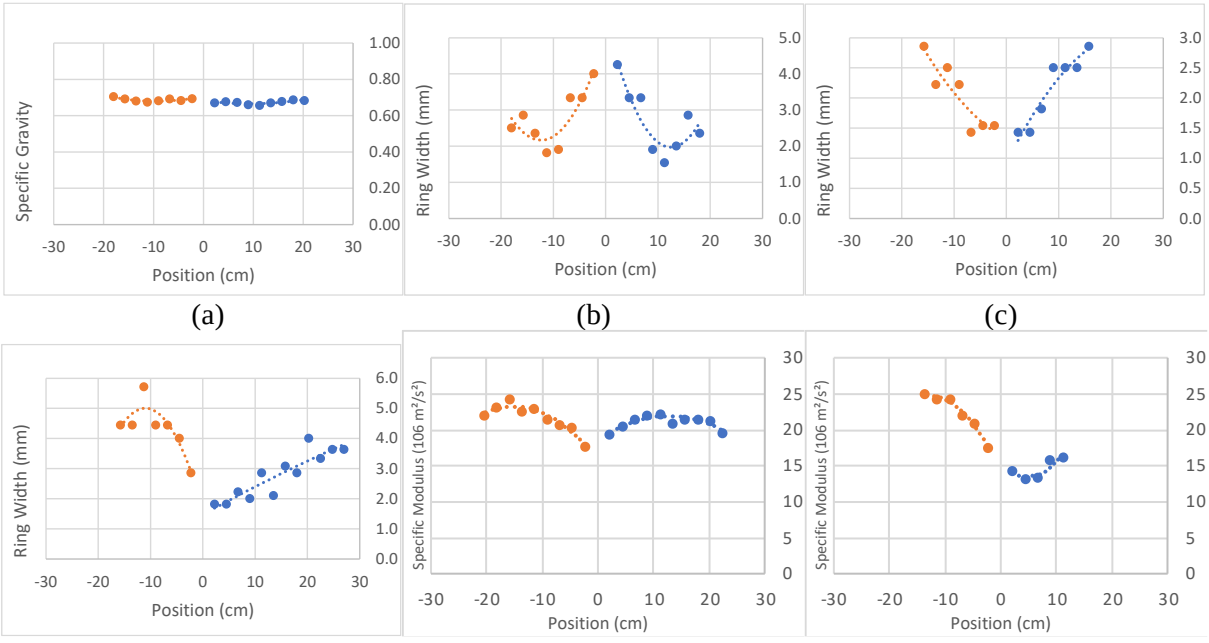


Fig. 5. Examples of property profiles: (a) tree 694, plot 6; (b) tree 443, plot 4; (c) tree 290, plot 2; (d) tree 1050, plot 9; (e) tree 1025, plot 9; (f) tree 299, plot 2

### 3.3.2 Typology of profiles

For each of the three studied variables (*RW*, *SG* and *SM*) there was a large diversity of radial profiles, with instances of all nine possible combinations of slope ("Up", "Flat", "Down") and curvature ("Convex", "Straight", "Concave"). Nevertheless, the frequency of these different shapes differed (Table 11). The proportion of symmetric profiles ("Sym") is about one third, showing that most trees display substantial variations of properties around the periphery.

Table 11. Occurrence of profile types for 172 north and south cases

| N + S | Sym | Flat | Up | Down | Straight | Convex | Concave |
|---|---|---|---|---|---|---|---|
| *RW* | 36% | 41% | 18% | 41% | 36% | 37% | 27% |
| *SG* | 37% | 42% | 13% | 45% | 48% | 34% | 19% |
| *SM* | 28% | 42% | 37% | 20% | 28% | 10% | 62% |

The proportion of flat radial profiles was of about 40% for each variable. Most other profiles were decreasing for *RW* and *SG*, and increasing for *SM*. But less than 50% of flat profiles were straight, meaning that most flat profiles were either convex (for *RW* or *SG*), or concave (as for *SM*) (Fig. 6).

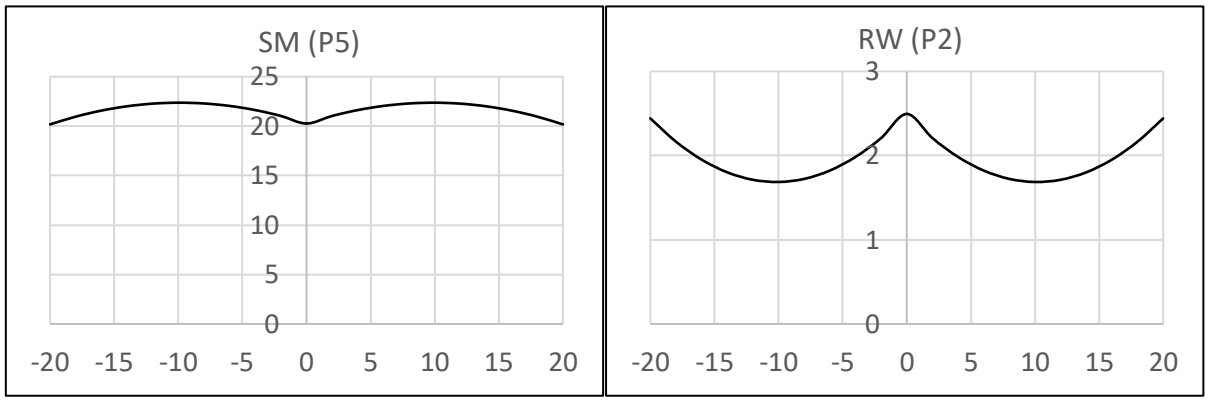


Fig. 6. Examples of median plot profiles with flat slope: flat-convex (*SM*, P5) or flat-concave (*RW*, P2)

The proportions of each type of profile seemed to differ between plots, as illustrated on Fig. 7.

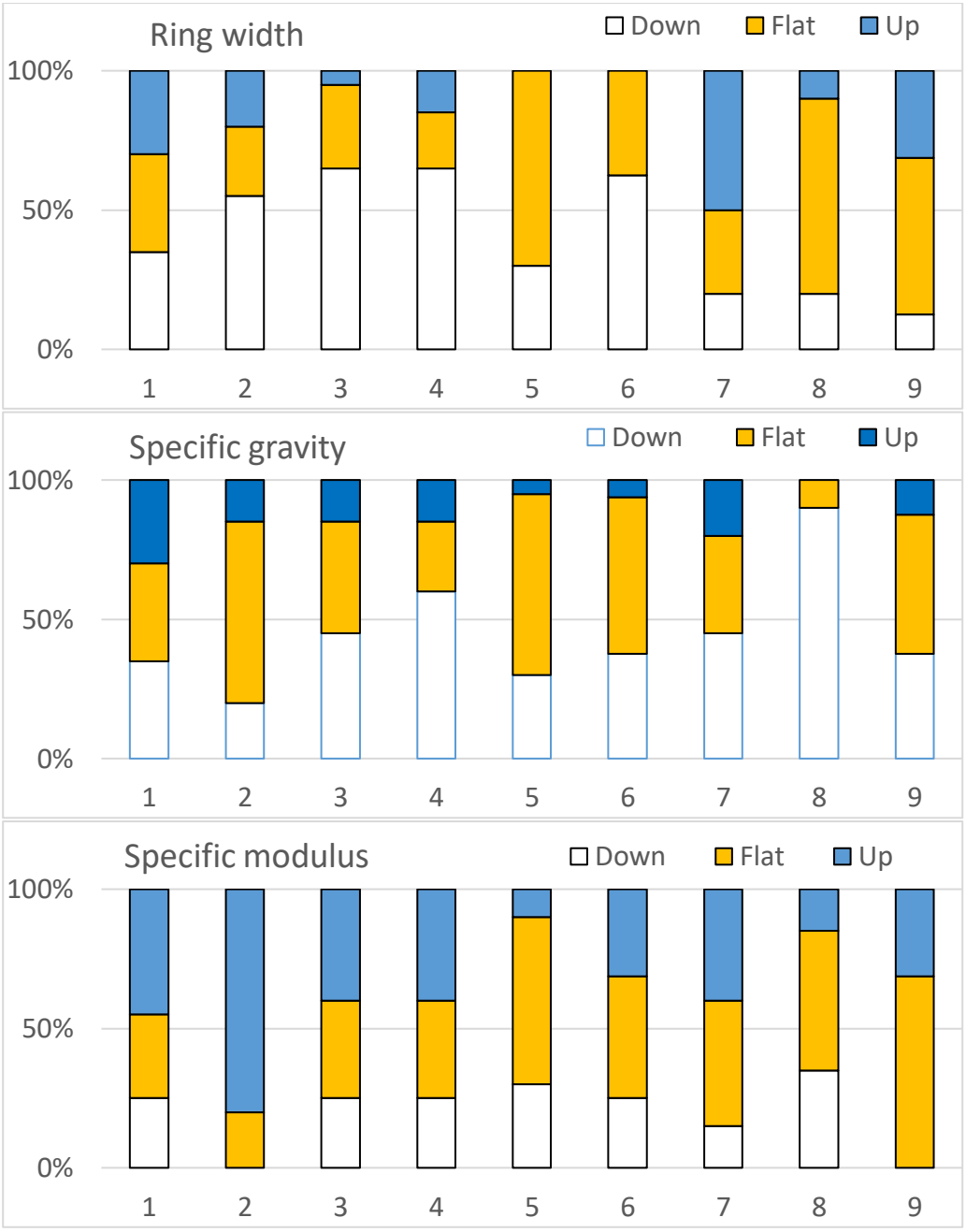


Fig. 7. Distribution of profile types per plot (based on the slope of linear regression)

### 3.3.3 Distribution of profiles shape parameters

The median shape of all radial profiles is illustrated on Fig. 8. These profiles were "down-convex" for *RW* and *SG*, and "up-concave" for *SM*. The shape of the median profile of each plot can be viewed from the supplementary material.

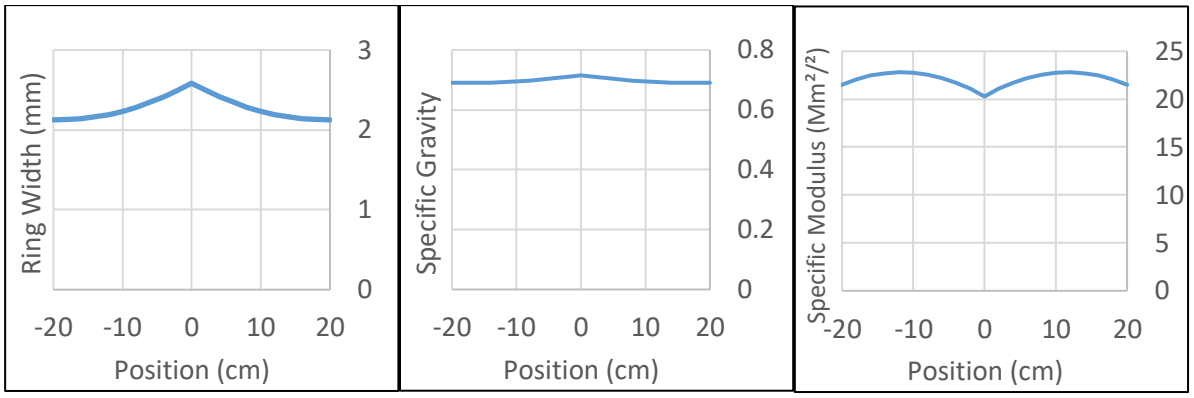


Fig.8 Median profiles over all trees, mixing both orientations in a symmetrical presentation.

The distribution of profile shape parameters is illustrated in Fig. 9. Each figure represents the distribution (median and inter-quartile) of parameters (slope and curvature) for each plot, together with "icons" illustrating the correspondence between the position on the graph and the profile shape. The figures are centred on zero on the X and Y axis, so that the centre of the figure represents the flat straight profile, and each quadrant of the figure represents a type of profile. A similar figure representing the distribution of parameter from individual radial profiles is provided in supplementary material.

It is apparent from Fig. 9 that shape parameters of profiles were not randomly distributed. The plot effect on the slope parameter was found significant for all three variables, while its effect on curvature was found significant only for *SG*.

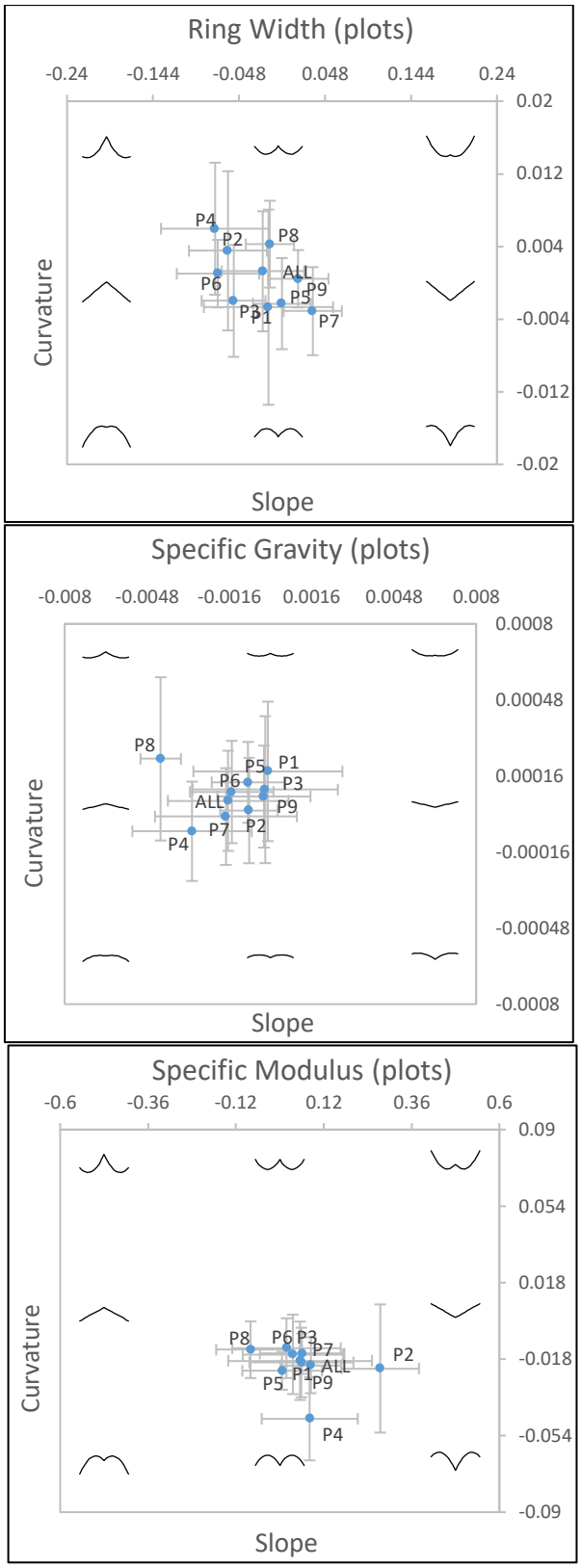


Fig. 9. Distribution of median plot profiles in the slope/curvature plane. Error bars represent the interquartile range of each plot. “Flying-bird” icons represent the shape associated to their position in the figure (see Fig. 4).

375 3.3.4 Correlations between profile shape parameters

376 The correlations between shape parameters of the profiles are illustrated in Fig. 10. The first
377 axis of this PCA opposed high initial ring width (*RW_a0*) and positive initial slope of specific
378 modulus (*SM_a1*) to high initial specific modulus (*SM_a0*) and positive slope of ring width
379 (*RW_a1*). This axis opposed high growth rate to high cell wall stiffness.

380 It is apparent that the initial slope (*_a1*) and curvature (*_a2*) were negatively correlated for all
381 three variables, meaning that the more the variable was initially quickly changing, the more this
382 rate of change was lowered during growth.

383

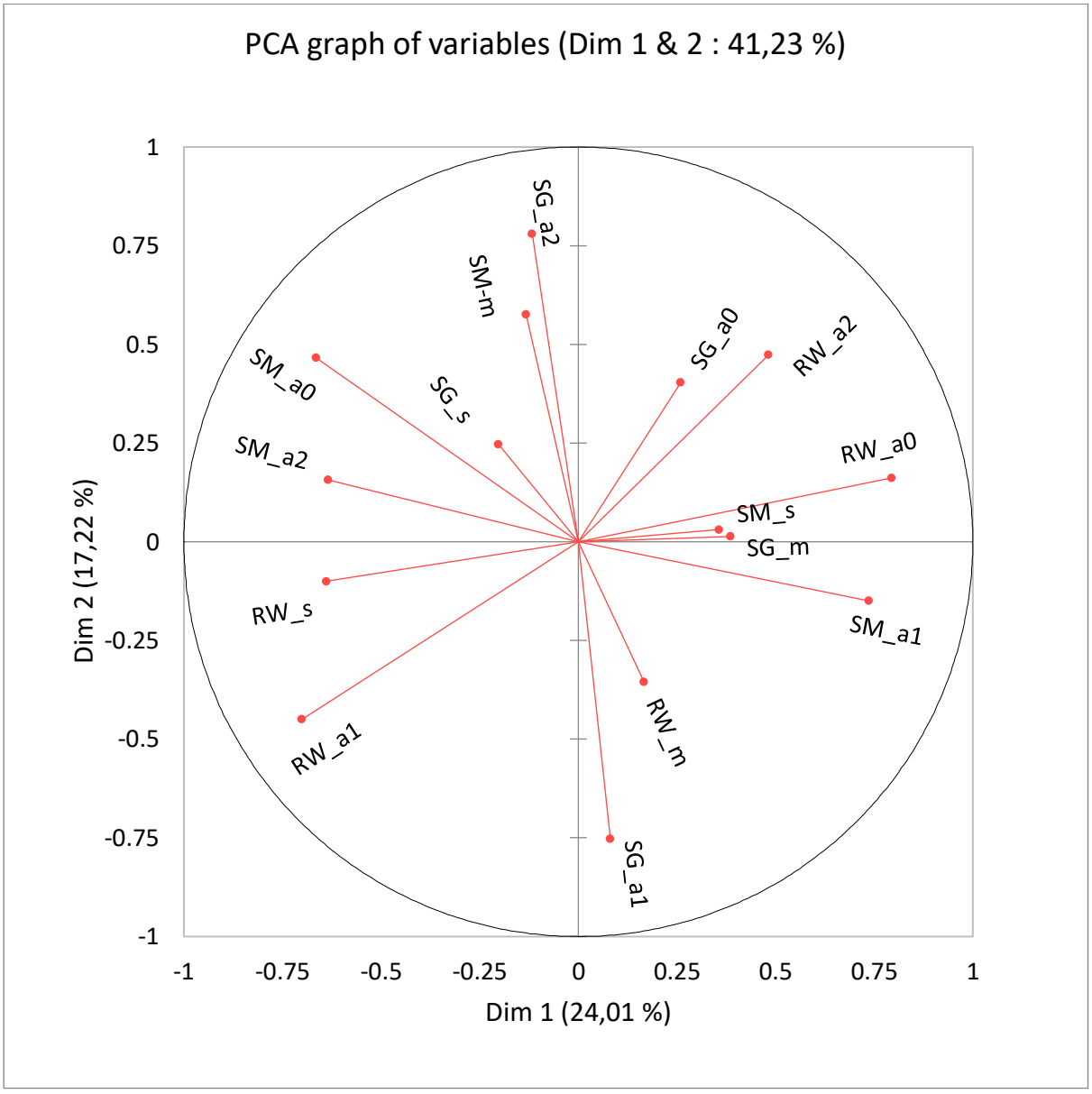


384

385 Fig. 10. Principal Component Analysis of shape profile parameters.
386 See §2.3.3 for the meaning of variables.

387

## 4. Discussion

### *4.1. Effect of red heartwood on wood properties*

Contrary to our expectations, the effect of red heartwood on the specific modulus was found significant, representing a substantial share of variance (8.6%). Its occurrence is associated to a lower *SM* (-0.67 $10^6$ m²/s² in average, 3% of the mean value), even when the effect of distance to the pith was accounted for. Pöhler et al (2006) found significant difference ($p<0.05$) both for density and modulus of elasticity. But the two parameters were higher for red heartwood (+3% and +6% respectively, which means +3% for *SM*). One reason for the difference could be due to a modification of cell wall properties during the expansion of red heartwood. Another one could be that trees with lower *SM* were more prone to develop read heartwood in our sampling. Anyway, in both studies, the difference between red heartwood and white heart density and specific modulus was quite small.

### *4.2. Interpretation of correlations between properties*

As a result of the large difference of variability between *SG* and *SM* (Table 5) the variability of the modulus of elasticity which is the product of *SG* and *SM*, is more dependent on the variations of *SM* than on the variations of *SG* in beech: The $R^2$ of the linear regression between MOE and SG is only 0.26, while that of the regression between SG and SM is 0.78.

Correlation between *RW* and both *SG* and *SM* were very highly significant, with a positive value for *SG* (density is higher for large ring width) and a negative one for *SM* (specific modulus is lower for large rings). These results were partly due to covariations along the juvenility gradient that will be analysed in the next paragraph.

There was no significant correlation between *SG* and *SM*. This can be interpreted as a global independence in mechanical adaptation of the two parameters: *SG* reflects the quantity of cell wall (cell wall relative thickness), and *SM* its quality (microfibril angle), and these two parameters can be regulated independently.

### *4.3. Major importance of within-tree variations in properties*

The importance of within-tree variations can be deduced from Table 3. Within-tree variation is the share of variance that is not captured by higher scale factors ("Plot" and "Tree"), so it is the sum of the "Core" factor, the "Orientation" factor and the "Error" factor (this last factor is not shown in Table 3, it is the differences between 100% and the sum of all displayed effects). Within-tree variations represented approximately 65% of variance for *RW*, 50% for *SG* and 55% for *SM*.

The within-tree variations of properties originated from both peripheral variations and radial variations. Peripheral variations were reflected by the frequent occurrence of non-symmetric diametral profiles: for all 3 studied variables, most trees presented important differences between North and South profiles (Table 11, Fig. 5). Radial variations were reflected by the importance of the "Core" effect (Table 3), and by the non-zero values of slope and curvature parameters of most radial profiles (section 3.3.3).

### *4.4. The frequency of non-symmetric diametral profiles reveals the importance of the gravity constraint and posture control mechanisms.*

Most diametral profiles were asymmetric (Table 11) despite the fact that the "Orientation" factor had no systematic effect on wood properties (Table 3). This is because the tree asymmetry, if any, due to stem inclination (linked to the effect of wind or soil instability), asymmetric crown (linked to the adaptation to light availability), and/or prevailing winds, had only few reasons to be North/South. It is thus not surprising to find insignificant systematic effect of orientation in the sampling.

The tree asymmetry induces mechanical constraints in relation to how trees manage gravity. The growth of an asymmetric tree induces a rapid increase of the bending moment applied by gravity of the trunk, which tends to bend the tree downwards. To counteract this effect, a gravitropic reaction is needed (Alméras & Fournier 2009, Gril et al 2017). This reaction is achieved by a dissymmetry of growth forces on the two sides of the inclined stem: a higher tensile force on the upper side for hardwood species like beech. The tensile force produced on each side of the tree during wood maturation process is proportional to ring width, to specific gravity, to specific modulus and to maturation strain (Alméras et al 2005, Thibaut et Gril 2021). Increasing the force on the upper side means increasing the local value of any combination of these four factors, together with decreasing it on the lower side. This leads to asymmetric profiles of wood properties.

Reaction wood occurrence is the typical expression of strong gravitropic reactions, influencing the asymmetry in *RW*, *SG*, *SM*, and the asymmetry in maturation strains, that results from macromolecular processes occurring during secondary wall formation (Alméras and Clair 2016, Thibaut and Gril 2021). However, for small inclination angles (e.g. coppice stems) the production of tension wood is not necessary: the difference in maturation strain between normal wood located on lower and upper sides of the growing stem can be high enough to enable posture control (Thibaut and Gril 2021). Tension wood occurrence is rather easy to detect by visual observation but variations of maturation strain in normal wood are, until now, impossible to estimate except by in-situ measurements of residual stress at stem periphery (Jullien et al 2013).

### *4.5. Diversity in radial profiles suggests that "adaptive juvenility" is prevailing over "ontogenetic juvenility"*

Most of the papers on mechanical properties of juvenile wood refer to plantation, either of softwoods or hardwoods (Bensend and Senft 1986, Kojima et al 2009, Bhat et al 2001, Bao et al 2001). For softwoods, the "typical radial pattern" (TRP) for mechanical factors (Lachenbruch et al 2011) is always the case for fast-growing plantations. It is characterized by a decrease of *RW* and an increase of both *SG* and *SM* from pith to bark until a juvenile core limit.

For hardwoods this is not always the case, and *SG* can be more or less flat (Bendtsen & Senft 1986), while *SM* can be high near the pith and decrease for trees growing in dense tropical forest (Mc Lean et al 2011). On *Bagassa guianensis*, a fast-growing secondary forest tree of French Guiana, Bossu et al (2018) observed a general TRP for microfibril angle and density, very clear for density (varying from 0.3 to 0.9 along the radius). Plourde et al (2015) studied radial density variation for 91 tropical species (Costa Rica): 42 over 74 had a net variation in density, 37 with increasing TRP type and 5 with decreasing "anti TRP" type. Secondary forest species (open environment in juvenile phase) had the clearest positive variations (low juvenile density), primary forest species (closed environment in juvenile phase) were the only anti-TRP species, with a lower variation (high internal density). Beech in this study is rather similar to trees from the primary forest with an internal density above 0.5 and a decreasing profile. Longuetaud et al (2017) studied 3 broadleaved trees: oak, beech, sycamore maple and two softwoods: fir and Douglas fir. The TRP model was valid for maple and Douglas fir, but for oak the density decreased instead of increasing. For fir and beech, the profile was bell-shaped (beech) or U-shaped (fir) with slight variations. Purba et al (2021) studied density and microfibril angle in oak and beech for dominated, small-diameter trees harvested during thinning. Overall, the TRP applied to both cases.

For beech, we have measured parameters describing the juvenility of old trees in managed forest with a rather large variety of plot environment and management practices. The median profiles

for each mechanical parameter (beech radial pattern in Fig. 8) was similar to some hardwood description in literature for *SG*.

In Europe, old growth beech forests can have different forest origins (Ciancio et al 2006): even-aged (France or Germany) or uneven-aged high forest (Switzerland), coppicing with standards (France) or conversion of coppice forest into high forest (Germany, France) but are very rarely the result of plantations (none in the 9 plots). *Fagus* is known for its shade tolerance and ability to grow very slowly under a closed canopy (Collet et al 2011) and most forest plots undergo more or less severe thinning before final harvesting, which leads to an increase of *RW* due to better access to light (Noyer et al 2017). This is reflected in the different mean *RW* radial patterns for the 9 plots (Fig. 9). For plots 7 (uneven-aged high forest) and 9 (middle forest transformed in even-aged high forest), a clear increase of *RW* was observed in the young ages, while the reverse and classical pattern was true for plots 1, 4, 5 and 6 (all even-aged forest in flat area). Similar results were found on younger beech trees (Bouriaud et al 2004). The low *RW* values for plots 2 and 8 (even aged, steep terrain) could be expected in a mountainous area, and the observed increase of *RW* after an initial decrease possibly due to thinning operations.

Probably due to the large diversity of plot management, the beech median radial pattern did not apply to many trees of the sampling. As a result, there was no "universal" juvenile trend for any of the 3 parameters for all trees. Combining global trend (flat, up, down) and curvature (straight, convex, concave), there was a large variety of profile occurrence in each of the 9 cross-types for each plot. This was similar to the large variety of radial patterns found in most of the studied hardwoods, contrary to the "universal" pattern for fibre (or tracheid length). Even if there is a part of ontogenetic influence in the juvenile patterns for *RW*, *SG* and *SM*, the results suggest the main influence of plastic adaptation to mechanical constraints in the tree growth (adaptive juvenility).

## 5. Conclusion

Based on the analysis of variance and the analysis of radial profiles, we showed that, for the 3 studied variables (*RW*, *SG* and *SM*) within-tree variations represented the largest part of variance. These within-tree variations occurred both through peripheral variations (asymmetry between North and South profiles) and through radial variations (dependence of the property on the distance to the pith). The patterns of radial variations of the 3 variables were diverse, including increasing, flat and decreasing patterns, as well as convex, straight and concave patterns. Overall, these observations demonstrate that juvenile wood in Beech did not obey to systematic variations (ontogenetic juvenility), but was the result of plastic adaptation (adaptive juvenility) to variable individual trajectories and associated mechanical constraints.

## Acknowledgments

The data were obtained thanks to the support of European Commission through the FAIR-project CT 98-3606, coordinated by Prof. Gero Becker. The financial support of CNRS K. C. Wong post-doctoral program and China Scholarship Council must be also acknowledged.

## References

Alméras T, Thibaut A, Gril J. 2005. Effect of circumferential heterogeneity of wood maturation strain, modulus of elasticity and radial growth on the regulation of stem orientation in trees. Trees 19 (4), 457-467. https://doi.org/10.1007/s00468-005-0407-6

Alméras T., Fournier M. 2009. Biomechanical design and long-term stability of trees: Morphological and wood traits involved in the balance between weight increase and the

gravitropic reaction. Journal of Theoretical Biology 256: 370–381. https://doi.org/10.1016/j.jtbi.2008.10.011

Alméras T, Clair B. 2016. Critical review on the mechanisms of maturation stress generation in trees. Journal of the Royal Society, Interface 13(122), 20160550. https://doi.org/10.1098/rsif.2016.0550

Bao FC, Jiang ZH, Jiang XM, Lu XX, Luo XQ, Zhang SY. 2001. Differences in wood properties between juvenile wood and mature wood in 10 species grown in China. Wood Science and Technology 35:363-375. https://doi.org/10.1007/s002260100099

Bar-On YM, Phillips R, Milo R. 2018. The biomass distribution on Earth. Proceedings of the National Academy of Sciences, 115(25), 6506-6511. https://doi.org/10.1073/pnas.1711842115

Bhat KM, Priya PB, Rugmini P. 2001. Characterisation of juvenile wood in teak. Wood Science and Technology 34:517-532. https://doi.org/10.1007/s002260000067

Becker G, Beimgraben T. 2001. Occurrence and relevance of growth stresses in Beech (Fagus sylvatica L.) in Central Europe. Final Report of FAIR-project CT 98-3606, Coordinator Prof. G. Becker, Institut für Forstbenutzung und forstliche Arbeitwissenschaft, Albert-Ludwigs Universität, Freiburg, Germany.

Bendtsen BA, Senft J. 1986. Mechanical and anatomical properties in individual growth rings of plantation-grown eastern cottonwood and Loblolly pine. Wood and Fiber Science 18(1): 23-38.

Bossu J, Lehnebach R, Corn S, Regazzi A, Beauchene J, Clair B. 2018. Interlocked grain and density patterns in *Bagassa guianensis*: changes with ontogeny and mechanical consequences for trees. Trees - Structure and Function, 32(6):1643-1655. https://doi.org/10.1007/s00468-018-1740-x.

Bouriaud O, Bréda N, Le Moguédec G, Nepveu G. 2004. Modelling variability of wood specific gravity in beech as affected by ring age, radial growth and climate. Trees 18:264–276. https://doi.org/10.1007/s00468-003-0303-x

Brancheriau L, Baillères H. 2002. Natural vibration analysis of wooden beams: a theoretical review. Wood Science and Technology, 36(4):347-365. https://doi.org/10.1007/s00226-002-0143-7

Cave ID. 1969. The Longitudinal Young's Modulus of *Pinus Radiata* Wood Science and Technology, Vol. 3, p. 40-48

Ciancio O, Corona P, Lamonaca A, Portoghesi L, Travaglini D. 2006. Conversion of clearcut beech coppices into high forests with continuous cover: A case study in central Italy. Forest Ecology and Management 224: 235–240. https://doi.org/10.1016/j.foreco.2005.12.045

Collet C, Fournier M, Ningre F, Hounzandji AP, Constant T. 2011. Growth and posture control strategies in Fagus sylvatica and Acer pseudoplatanus saplings in response to canopy disturbance. Annals of Botany 107, 1345–1353. https://doi.org/10.1093/aob/mcr058

Cown D, Dowling L. 2015. Juvenile wood and its implications. NZ Journal of Forestry, February 2015, Vol. 59, No. 4: 10-17

Dassot M, Constant T, Ningre F, Fournier M. 2015. Impact of stand density on tree morphology and growth stresses in young beech (Fagus sylvatica L.) stands. Trees, https://10.1007/s00468-014-1137-4

Déjardin A, Laurans F, Arnaud D, Breton C, Pilate G, Leplé JC. 2010. Wood formation in Angiosperms. C. R. Biologies 333 (2010) 325–334.

Dlouhá J, Alméras T, Beauchêne J, Clair B, Fournier M. 2018. Biophysical dependences among functional wood traits. Functional Ecology, 32(12), 2652-2665. https://doi.org/10.1111/1365-2435.13209

572 Fournier M, Dlouha J, Jaouen G, Alméras T. 2013. Integrative biomechanics for tree ecology:
573 beyond wood density and strength. Journal of Experimental Botany, 64(15), 4793-4815.
574 https://doi.org/10.1093/jxb/ert279

575 Gril J, Jullien D, Bardet S, Yamamoto H. 2017. Tree growth stress and related problems.
576 Journal of Wood Science, 63 (5), 411-432. https://doi.org/10.1007/s10086-017-1639-y

577 Jullien D, Widmann R, Loup C, Thibaut B. 2013. Relationship between tree morphology and
578 growth stress in mature European beech stands. Annals of forest science 70 (2), 133-142.
579 https://doi.org/10.1007/s13595-012-0247-7

580 Kojima M, Yamamoto H, Yoshida M, Ojio Y, Okumura K. 2009. Maturation property of fast-
581 growing hardwood plantation species: A view of fiber length. Forest Ecology and Management
582 257: 15–22. https://doi.org/10.1016/j.foreco.2008.08.012

583 Kollmann FFP, Côté AA. 1968. Principles of wood Science and Technology, I. Solid Wood,
584 Springer-Verlag, New York. https://link.springer.com/book/10.1007/978-3-642-87928-9

585 Koubaa A, Hernandez RE, Baudouin M, Poliquin J. 1998. Inter clonal, intra clonal and within-
586 tree variation of fiber length of poplar hybrid clones. Wood and Fiber Science 30(1): 40-47

587 Kretschmann DE. 2010. Mechanical properties of wood. In Wood handbook: Wood as an
588 engineering material. General Technical Report FPL-GTR-190. Madison: Forest Products
589 Laboratory, USDA, Forest Service.

590 Lachenbruch B, Moore J, Evans R. 2011. Radial variation in wood structure and function in
591 woody plants, and hypotheses for its occurrence. In: Meinzer FC, Lachenbruch B, Dawson TE
592 (eds) Size- and age-related changes in tree structure and function. Springer, Dordrecht: 121–
593 164.

594 Larson PR, Kretschmann DE, Clark AIII, Isebrands JG. 2001. Formation and properties of
595 juvenile wood in southern pines: a synopsis. Gen. Tech. Rep. FPL-GTR-129. Madison, WI:
596 U.S. Department of Agriculture, Forest Service, Forest Products Laboratory. 42 p.

597 Longuetaud F, Mothe F, Santenoise P, Diop N, Dlouha J, Fournier M, Deleuze C. 2017. Patterns
598 of within-stem variations in wood specific gravity and water content for five temperate tree
599 species. Annals of Forest Science 74:64. https://doi.org/10.1007/s13595-017-0657-7

600 Loup C, Fournier M, Chanson B. 1991. Relations entre architecture mécanique et anatomie de
601 l'arbre : cas d'un Pin Paritime (*Pinus pinaster* Soland.). L'arbre, biologie et développement.
602 Naturalia monspeliensa N° hors série (C. Edelin ed)

603 Liu S, Loup C, Gril J, Dumonceaud O, Thibaut A, Thibaut B. 2005. Studies on European beech
604 (Fagus sylvatica L.): variations of colour parameters. Annals of Forest Science, 62: 625-632.
605 https://doi.org/10.1051/forest:2005063

606 Mc Lean JP, Zhang T, Bardet S, Beauchêne J, Thibaut A, Clair B, Thibaut B. 2011. The
607 decreasing radial wood stiffness pattern of some tropical trees growing in the primary forest is
608 reversed and increases when they are grown in a plantation. Annals of Forest Science 68: 681-
609 688. https://doi.org/10.1007/s13595-011-0085-z

610 Noyer E, Lachenbruch B, Dlouhá J, Collet C, Ruelle J, Ningre F, Fournier M. 2017. Xylem
611 traits in European beech (Fagus sylvatica L.) display a large plasticity in response to canopy
612 release. Annals of Forest Science 74: 46, https://doi.org/10.1007/s13595-017-0634-1

613 Plourde BT, Boukili VK, Chazdon RL. 2015. Radial changes in wood specific gravity of
614 tropical trees: inter- and intraspecific variation during secondary succession. Functional
615 Ecology, 29:111–120. https://doi.org/10.1111/1365-2435.12305

Pöhler E, Klingner R, Künniger T. 2006. Beech (Fagus sylvatica L.) – Technological properties, adhesion behaviour and colour stability with and without coatings of the red heartwood. Ann. For. Sci. 63 (2006) 129-137. https://doi.org/10.1051/forest:2005105

Purba CYC, Dlouha J, Ruelle J, Fournier M. 2021. Mechanical properties of secondary quality beech (Fagus sylvatica L.) and oak (Quercus petraea (Matt.) Liebl.) obtained from thinning, and their relationship to structural parameters. Annals of Forest Science 78: 81. https://doi.org/10.1007/s13595-021-01103-x

R Core Team 2018. R: A language and environment for statistical computing. R Foundation for Statistical Computing, Vienna, Austria.

Raven PH, Evert RF, Eichhorn SE. 2007. The biology of plants. Brussels: De Boeck.

Ross, R. J. (2010). Wood handbook: wood as an engineering material. USDA Forest Service, Forest Products Laboratory, General Technical Report FPL-GTR-190, 2010: 509 p. 1 v., 190.

Savidge RA. 2003. Tree growth and wood quality. In: Wood quality and its biological basis, edited by JR. Barnett and G. Jeronimidis, Blackwell scientific, Oxford, UK (ISBN: 978-1-405-14781-1): 1-29

Thibaut B. 2019. Three-dimensional printing, muscles and skeleton: mechanical functions of living wood. Journal of Experimental Botany, Volume 70, Issue 14, 1 July 2019, Pages 3453–3466. https://doi.org/10.1093/jxb/erz153

Thibaut B, Gril J. 2021.Tree growth forces and wood properties. Peer Community Journal, Volume 1, article no. e46. https://doi.org/10.24072/pcjournal.48

Trenčiansky M, Lieskovský M, Merganič J, Šulek R (2017). Analysis and evaluation of the impact of stand age on the occurrence and metamorphosis of red heartwood. iForest 10: 605-610. – doi: 10.3832/ifor2116-010 [online 2017-05-15]